ELSEVIER

Biochimica et Biophysica Acta 1467 (2000) 73–84

BIOCHIMICA ET BIOPHYSICA ACTA
BBA

www.elsevier.com/locate/bba

Requirement of the hinge domain for dimerization of Ca^{2+}-ATPase large cytoplasmic portion expressed in bacteria

Paulo C. Carvalho-Alves, Vitor R. Hering, Juliana M.S. Oliveira, Roberto K. Salinas, Sergio Verjovski-Almeida *

Departamento de Bioquímica, Instituto de Química, Universidade de São Paulo, Caixa Postal 26077, 05513-970 São Paulo, SP, Brazil

Received 13 December 1999; received in revised form 14 March 2000; accepted 21 March 2000

Abstract

The large cytoplasmic domain of rabbit sarcoplasmic reticulum Ca^{2+}-ATPase was overexpressed in *Escherichia coli* as a 48 kDa fusion protein, designated p48, containing an N-terminal hexa-His tag. Purification conditions were optimized, thus conferring long-term stability to p48. Circular dichroism spectroscopy and the pattern of limited trypsinolysis confirmed the proper folding of the domain. p48 retained 0.5 ± 0.1 mol of high affinity 2′,3′-*O*-(2,4,6-trinitrophenyl)adenosine-5′-triphosphate (TNP-ATP) binding sites per mol of polypeptide chain with an apparent dissociation constant of about 8 μM. Size-exclusion FPLC using protein concentrations in the range 0.03–5 mg/ml showed that p48 was essentially monodisperse with apparent molecular mass and Stokes radius (R_s) values compatible with a dimer (100 kDa and 40 Å, respectively). Analysis of p48 by small-angle X-ray scattering provided an independent second proof for a dimeric p48 particle with a radius of gyration (R_g) of 39 Å, suggesting that the dimer was not spherical ($R_s/R_g = 1.026$). When digested by proteinase K, p48 was converted to a 30 kDa fragment, designated p30, which was very resistant to further proteolysis. p30 retained high affinity TNP-ATP binding ($K_d = 8$ μM) and eluted as a monomer (35 kDa) in size-exclusion FPLC. As opposed to p48, the p30 fragment did not react with monoclonal antibody A52 [Clarke et al., J. Biol. Chem. 264 (1989) 11246–11251] which recognizes region E657–R672 located upstream of the hinge domain of the Ca^{2+}-ATPase. These results indicate a requirement of the hinge domain (670–728) region for self-association of the p48 large hydrophilic domain as a dimer. We propose that this behavior points to a possible role of the hinge domain in dimerization of sarcoplasmic reticulum Ca^{2+}-ATPase in the native membrane.

Keywords: Sarcoplasmic reticulum Ca^{2+}-ATPase; Bacterial heterologous expression; Hexa-histidine tag; Nickel affinity chromatography; Circular dichroism; Fluorescence; Small-angle X-ray scattering; Limited proteolysis

1. Introduction

Sarcoplasmic reticulum Ca^{2+}-ATPase belongs to the class of P-type transmembrane ion transport proteins, which forms a phosphoprotein intermediate during the reaction cycle [1]. Ca^{2+}-ATPase consists of a single polypeptide chain of 997 amino acid residues. The most likely tertiary structure arrangement comprises a small and a large cytoplasmic domain

Abbreviations: FPLC, fast protein liquid chromatography; CD, circular dichroism; SAXS, small-angle X-ray scattering; TNP-ATP, 2′,3′-*O*-(2,4,6-trinitrophenyl)adenosine-5′-triphosphate

* Corresponding author. Fax: +55-11-3818-2186; URL: http://www.iq.usp.br/wwwchem/bioquimica/;
E-mail: verjo@iq.usp.br

0005-2736/00/$ – see front matter
PII: S0005-2736(00)00206-6

separating three clusters of transmembrane segments [2]. The membrane topology has been confirmed by recent progress in crystallization that produced low resolution atomic models of sarcoplasmic reticulum Ca^{2+}-ATPase [3,4]. Early kinetic studies of ATP hydrolysis showed a biphasic dependence of the activity on substrate concentration [1,5] which has been attributed to a dimeric structure of the enzyme, although it has been pointed out that the biphasic kinetics is similarly consistent with a monomeric enzyme that converts between two forms with different affinities for substrate [6]. The tendency of Ca^{2+}-ATPase to self-associate into a dimer has been characterized by physico-chemical methods of analysis of both solubilized [7–9] and membrane-bound ATPase [10,11], although fully active monomeric Ca^{2+}-ATPase has been described [12]. The role of dimeric protein–protein interactions in regulating the kinetic mechanism of Ca^{2+}-ATPase has been emphasized [13].

Several functional sites have been identified in the large hydrophilic domain of Ca^{2+}-ATPase by affinity labeling experiments [14,15]. The large hydrophilic domain is predicted to be situated between Met326 and Ile743, containing 42% of the amino acids of the protein. It contains five of the seven most highly conserved sections of the P-type ATPase sequences. The NH_2-terminal part of the large domain comprises the aspartyl residue 351 that is phosphorylated by ATP during the catalytic cycle. In addition, the large domain contains nucleotide binding motifs and contains the so-called hinge domain in its carboxy-terminal portion (residues 670–728) [14,16].

The relative contribution of either hydrophilic or hydrophobic domains for self-association has never been investigated, probably because of the present difficulties in generating recombinant full-length Ca^{2+}-ATPase with a degree of purity and in amounts that would be adequate for physico-chemical studies. In order to circumvent these limitations, we have opted to analyze self-association using only the recombinant large hydrophilic domain. The bacterial expression and purification of the whole hydrophilic large cytoplasmic domain of sarcoplasmic reticulum ATPase previously described by Moutin et al. [17,18] was used. In the present report, expression and purification with high yields of p48, a Ca^{2+}-ATPase fragment comprising the whole hydrophilic large cytoplasmic domain of sarcoplasmic reticulum ATPase (residues 326–743), was obtained and conditions for long-term stability of the recombinant protein have been optimized. Proper folding of p48 was investigated using circular dichroism (CD) spectroscopy, limited proteolysis with trypsin or proteinase K and 2′,3′-*O*-(2,4,6-trinitrophenyl)adenosine-5′-triphosphate (TNP-ATP) binding affinity. A limited number of cleavage sites suggested that p48 has a folding which is similar to the native domain of membrane-bound ATPase. Size-exclusion fast protein liquid chromatography (FPLC) and small angle X-ray scattering (SAXS) showed that p48 was a monodisperse dimeric particle. Interestingly, digestion of p48 with proteinase K converted the protein to a 30 kDa fragment (p30) which we showed to be monomeric and to be devoid of the conserved hinge domain located at the carboxy-terminal portion of p48. p30 obtained in the present study is essentially similar to the proteolysis-resistant core fragment p29/p30 produced by proteinase K digestion of membrane-bound native ATPase [19], which was similarly shown to be monomeric and devoid of the hinge domain [19]. Taken together, our data indicate that the conserved hinge domain drives self-association of p48 into a dimer, and suggest that the hinge domain may play a role in dimerization of Ca^{2+}-ATPase in the native sarcoplasmic reticulum membrane.

2. Materials and methods

2.1. Sarcoplasmic reticulum Ca^{2+}-ATPase clone

The cDNA of rabbit adult fast-twitch muscle sarcoplasmic reticulum Ca^{2+}-ATPase (SERCA1) cloned into plasmid pBSfA was used [20].

2.2. Amplification of two DNA sequences by PCR

Portions of the cDNA of sarcoplasmic reticulum Ca^{2+}-ATPase corresponding to the large cytoplasmic domain were amplified by PCR using the following primers: 5′ primer CCG CTC GAG ATG GCG AAG AAG AAC GCC ATC G corresponding to the SERCA1 sequence encoding amino acids 326–333; 3′ reverse primer ACG GCT CGA GGA TGG TGG AGA AGT TGT CGT CC correspond-

ing to the SERCA1 sequence encoding amino acids 743–737. PCR product was cloned into the *Xho*I restriction site of pBluescript (Stratagene, La Jolla, CA, USA) and sequenced in an automated sequencer to confirm that no mutations were present.

2.3. Construction of the expression vectors

The sequence was extracted from pBluescript and cloned in the bacterial expression vector pProEx-1 (Gibco BRL, Gaithersburg, MD, USA) in the *Xho*I restriction site generating the vector pProEx/Large. The direction of insertion was checked by restriction digestion. pProEx-1 expresses the recombinant DNA as a fusion protein containing a hexa-histidine tag at the amino-terminal end. Expression of the large cytoplasmic domain was extremely low in the pProEx-1 system using the conditions recommended by the manufacturer. The large domain sequence was extracted from pProEx/Large in two fragments, *Bam*HI–*Bam*HI and *Bam*HI–*Hin*dIII. The latter was cloned into pQE9. Subsequently the *Bam*HI–*Bam*HI fragment was added, and the orientation was checked by restriction digestion generating vector pQE/Large. pQE9/Large expresses the recombinant DNA as a fusion protein containing the hexa-histidine tag construction which was carried from the pProEx-1 vector at the amino-terminal end of the SERCA1 large cytoplasmic domain spanning from M326 to I743.

2.4. Expression in Escherichia coli

Vector pQE/Large was used to transform *E. coli* strain M15 (Qiagen, Santa Clarita, CA, USA) already transformed with the pREP4 plasmid (Qiagen). *E. coli* transformants were selected on LB agar containing ampicillin (100 μg/ml) and kanamycin (25 μg/ml). An overnight culture of 10 ml was prepared, and used for inoculating 1 l of LB medium enriched with 10 mM KCl, 4 mM $MgSO_4$ containing 100 μg/ml ampicillin and 25 μg/ml kanamycin, and incubated with shaking at 37°C. Expression was induced after 135 min by adding 1.5 mM IPTG (isopropyl-1-thio-β-D-galactopyranoside). Bacteria were further grown for 150 min. Cells were then centrifuged at $5000\times g$ for 10 min, the supernatant was drained and the pellets were frozen at −80°C.

2.5. Extraction with urea and purification

Cells expressing the large domain were brought from −80°C to an ice bath for 10 min. To each 250 ml of culture pellet 10 ml of lysis buffer (50 mM NaH_2PO_4, 1 mM phenylmethylsulfonyl fluoride (PMSF), pH 7) was added to resuspend the cells. Cell lysis was performed in a French press with 16 000 psi pressure. The extract was centrifuged at $10\,000\times g$ for 10 min at 4°C and the supernatant was discarded. The pellet was suspended in 10 ml of extraction buffer (6 M urea, 25 mM sodium phosphate, 200 mM $(NH_4)_2SO_4$, pH 7.5, 10 mM β-mercaptoethanol) and centrifuged at $10\,000\times g$ for 10 min. The supernatant was collected and used to load the affinity column.

A 15 ml column was charged with 4 ml of Ni-NTA resin (Ni^{2+}–nitrilotriacetic acid–agarose; Qiagen) equilibrated with extraction buffer and loaded in batch mode with 10 ml of the supernatant extract. After 5–10 min of incubation the column was drained and washed twice with 10 ml of extraction buffer, once with 10 ml of extraction buffer supplemented with 25 mM imidazole. The protein was then eluted as 1 ml samples with 10 ml of extraction buffer supplemented with 120 mM imidazole. Tubes containing protein were pooled and used for the subsequent step of gel filtration through a 120×3.5 cm Superose 12 (Pharmacia Biotech) column equilibrated with the extraction buffer. Fractions of 2.5 ml were collected and samples were analyzed by denaturing polyacrylamide gel electrophoresis (SDS–PAGE) to detect those enriched in the 48 kDa band (p48). Fractions were pooled (usually 15 ml) and used in the next step.

2.6. Dialysis and concentration

Standard dialysis procedures for p48 were performed in three steps of decreasing concentrations of urea for 12 h each at 4°C, against solutions containing 25 mM sodium phosphate pH 7.4, 10 mM β-mercaptoethanol, 3 mM dithiothreitol (DTT), 200 mM $(NH_4)_2SO_4$ (standard medium) and 4 M, 2 M or no urea. Under these conditions no protein aggregation was observed. Other salt contents and glycerol in the dialysis steps were tried and are briefly described in Section 4. After dialysis the protein was

stored on ice. Alternatively, the protein was concentrated 10-fold using an Ultrafree-15 centrifugal filter device (Millipore, Bedford, MA, USA) and the buffer could be changed to 20 mM MOPS at the same pH and in the presence of the same salt and reducing agents.

2.7. Protein characterization, trypsin digestion and immunoblot

Protein concentration for p48 was determined spectrophotometrically, using $\varepsilon_{280} = 16\,890$ M^{-1} cm^{-1}, as determined from its amino acid content using the Wisconsin GCG package (Genetics Computer Group, Madison, WI, USA) and confirmed by the Lowry method [21]. Limited trypsinolysis was performed by incubating 3 mg/ml p48 in 20 mM Tris–HCl pH 7, 100 mM KCl, 1 M sucrose in the presence of 37.5 μg/ml of trypsin at room temperature. The reaction was stopped by adding 5 mg of soybean inhibitor/mg of trypsin. Aliquots containing 12 μg of p48 were used for SDS–PAGE, using 15% polyacrylamide [22]. Gels were stained with Coomassie blue for protein. For partial digestion with proteinase K, 1 mg/ml p48 was incubated at room temperature for 10–40 min in the standard medium. The reaction was started upon the addition of 15 μg/ml proteinase K and arrested by the addition of 1 mM PMSF. Aliquots corresponding to 20 μg of the original p48 protein were used for SDS–PAGE [22]. Gels were stained with Coomassie blue. For Western blotting, protein was electro-transferred from gels to nitrocellulose membranes (Amersham, Buckinghamshire, UK) which were processed essentially as described by Harlow and Lane [22] using the mouse A52 anti-Ca^{2+}-ATPase monoclonal antibody [23] diluted 1/7000 or mouse anti-hexahistidine antibody (Sigma). Antibodies were detected using the ECL kit (Amersham, Buckinghamshire, UK) based on light emission by oxidation of luminol and sensitization of film (Hyperfilm/Amersham, Buckinghamshire, UK).

2.8. TNP-ATP fluorescence measurements

TNP-ATP fluorescence measurements were performed at room temperature in a medium containing 20 mM MOPS pH 7.25, 3 mM DTT, 100 mM KCl or 0.2 M $(NH_4)_2SO_4$, in a 1×1 cm fluorescence cuvette under continuous stirring using the photocounting spectrofluorimeter ISS PC1. The excitation wavelength was 410 nm (bandwidth = 5 nm) and the emission wavelength was 540 nm (bandwidth = 20 nm). Nucleotide binding was measured by the difference of fluorescence intensity in the presence and in the absence of p48 corrected for inner filter effect, as described by Moutin et al. [17].

2.9. CD spectroscopy

CD spectra were measured using a Jobin Yvon CD6 spectropolarimeter. Measurements were performed at room temperature (19°C) in 0.020 cm or 0.01 cm circular cells. Three scans from 190 to 260 nm were performed to obtain each spectrum. The units are expressed as molar ellipticity per residue (degree cm^2 $dmol^{-1}$).

2.10. CD spectrum deconvolution and secondary structure prediction

Three deconvolution algorithms were utilized as suggested by Greenfield [24]. The algorithms used were: Selcon containing 33 proteins in the data base [24,25], Contin using 16 proteins in the data base [26], and K2D neural network algorithm [27]. Secondary structure prediction was performed by the Predict Protein algorithm [28], or according to Chou and Fasman [29] using the GCG package (Genetics Computer Group).

2.11. Size-exclusion chromatography

p48 preparations and proteinase K-digested p30 samples were analyzed by size-exclusion FPLC (Model LCC 501 plus, Pharmacia Biotech) using a 30 ml Superose 12 column (Pharmacia Biotech) equilibrated with 25 mM sodium phosphate/0.2 M $(NH_4)_2SO_4$ buffer at pH 7.4, 10 mM β-mercaptoethanol, and in the presence of 3 mM DTT. The column was calibrated with standard proteins: aldolase, albumin, hemoglobin, ovalbumin and carbonic anhydrase using molecular masses and Stokes radii found in the literature [30].

2.12. SAXS of p48

SAXS experiments were performed at the National Laboratory of Synchrotron Light (LNLS), Campinas, Brazil, with the technical assistance of Mr. Guinther Kellerman and the supervision of Dr. Iris Torriani. Solutions of 4 mg/ml p48 in phosphate/ammonium sulfate buffer and 200 mM DTT were placed in 80 μl cells of 1 mm pathway in the absence or presence of 50 mM $MgCl_2$. Lower protein concentrations were tested and the results obtained were similar. Samples were exposed to 1.6 Å X-rays beam of a Synchrotron radiator for 10–20 min at room temperature. The intensity data were corrected for background (collected under identical conditions but without protein) and for sample absorption. The decay data were fitted with a sum of two exponential decays and the fitting was used for calculating radii of gyration (R_g) by the Guinier [31] approximation: $I(Q) = I(0)\exp(-R_g^2Q^2/3)$, where Q and $I(0)$ are the momentum transfer vector and the scattering intensity at zero scattering angle, respectively.

3. Results

3.1. p48 cytoplasmic domain has a native-like fold

The large cytoplasmic domain of Ca^{2+}-ATPase, designated p48, was expressed in bacteria as a fusion protein with an hexa-histidine N-terminal tag as originally described by the group of Dupont [17]. Essentially, the method consisted in solubilizing the inclusion bodies containing the expressed p48 protein with 6 M urea followed by purification through a Ni-NTA affinity column and refolding by removal of urea. A gel filtration step was introduced immediately following elution of p48 from the affinity column to ensure the removal of degradation products. In addition, a stepwise decrease in urea concentration was used, as described in Section 2. These proved to be critical steps in avoiding the previously reported loss of protein by aggregation during refolding [17] and in permitting long-term stability of refolded protein. The resulting purified p48 band accounts for more than 90% of proteins in the preparation, as seen on Coomassie blue-stained SDS–PAGE (Fig. 1A, lane 0), yielding about 15–25 mg of protein per liter of culture medium.

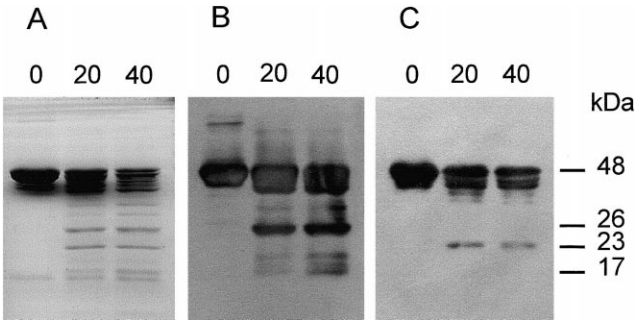

Fig. 1. Identification of amino and carboxy fragments of trypsin-digested p48. Gels were either (A) stained with Coomassie blue or developed by Western blot with either (B) monoclonal anti-Ca^{2+}-ATPase carboxy-end (E657–R672) or (C) anti-hexa-His amino-tag antibodies. Samples of 12 μg p48 were digested with trypsin for 0, 20 or 40 min as indicated and subjected to SDS–PAGE, as described in Section 2. The numbers on the far right indicate the calculated molecular mass of the major bands that accumulated at 20 min of digestion.

In order to test whether p48 had been folded in a similar way as the native ATPase, the pattern of partial digestion with trypsin was analyzed. Arginine 505–alanine 506 is well characterized as the most prominent site for limited trypsinolysis in sarcoplasmic reticulum Ca^{2+}-ATPase and is known as the T1 site. In the native protein, cleavage at T1 splits the ATPase in the middle of the large cytoplasmic domain, generating two fragments named A and B [32]. In p48 the corresponding arginine is at position 194 and cleavage at this site would produce two fragments, the amino-terminal with 21.4 kDa and the carboxy-terminal with 26.7 kDa. Fig. 1 shows that two main fragments of molecular mass around 23 kDa and 26 kDa accumulated within 20 min of digestion of p48 (Fig. 1A, lane 20), which is compatible with trypsinolysis occurring predominately at Arg194. In addition to the two fragments of 23 and 26 kDa a smaller amount of low molecular mass peptides of 17 and 15 kDa as well as non-resolved fragments between 48 and 44 kDa were also accumulated. Other high molecular mass peptides (30 and 40 kDa) were generated at longer times of digestion (Fig. 1A, lane 40).

Monoclonal antibodies have been used to identify the proteolytic fragments containing the C-terminal and N-terminal portions of p48. The C-terminal anti-

body A52 [23] recognizes the region E657–R672 located in the vicinity of the hinge domain of the Ca^{2+}-ATPase, and Fig. 1B shows that it reacted with the 26 kDa fragment, confirming that this band comprises the carboxy-terminal end of p48. The N-terminal antibody recognizes the hexa-His tag and Fig. 1C shows that it reacted with the 23 and not with the 26 kDa fragment, confirming that the 23 kDa band corresponds to the His-tagged amino-terminal fragment of p48. An important reactivity of monoclonal antibody A52 was observed at the 17 kDa band (Fig. 1B, lane 40), suggesting that it derived from further splitting of the 26 kDa fragment. This antibody also recognized the 40 kDa band (Fig. 1B, lanes 20 and 40), which was the result of cleavage at a less exposed additional site of trypsinolysis (see Fig. 1A, lane 40).

The immunoblotting results described above strongly suggest that the refolded p48 retained a native-like fold. The cleavage pattern is compatible with Arg194 being the most prominent trypsin cleavage site among the 54 potential trypsin sites contained in the large cytoplasmic domain, which corresponds to the T1 trypsin cleavage site of native ATPase.

3.2. Secondary Structure of p48

CD spectroscopy was employed (Fig. 2) in order to characterize p48 secondary structure content in the presence 0.2 M $(NH_4)_2SO_4$. Table 1 shows the results of CD spectrum deconvolution, using three different algorithms. It can be seen that the α-helix content obtained by CD spectral analysis was about 20–23% using the three algorithms, while the β-strand content was in the range of 21–25% with two of the algorithms and had an extreme value of 41% for the Contin 16 analysis. The fitting curve generated by K2D is shown in Fig. 2. The values generated by the K2D algorithm (Table 1) are similar to those found by Champeil et al. [19] for the p29/30 peptide obtained by digestion of native sarcoplasmic reticulum ATPase with proteinase K ($28 \pm 5\%$ α-helix and $20 \pm 3\%$ β-structure) and contains 60% the large hydrophilic domain (corresponding to p48 segment S39–S299).

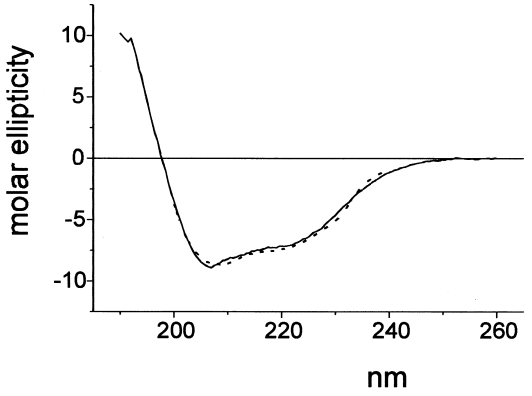

Fig. 2. CD spectrum of p48 at 340 μg protein/ml in 25 mM sodium phosphate buffer, containing 0.2 M ammonium sulfate, 10 mM β-mercaptoethanol, 3 mM DTT and 1 mM azide, at pH 7.4. The solid line shows the original smoothed spectrum, and the dashed line shows the fitting generated by the K2D algorithm. Molar ellipticity is in deg cm^2 $dmol^{-1}$.

Table 1
Secondary structure content of p48 obtained by CD spectral deconvolution

Secondary structure motif	Selcon 33	Contin 16	K2D[b]
Alpha-helix (%)	20	21 ± 1	23
Beta-strand (%)	25	41 ± 2	21
Other (%)	54	$37^a \pm 3.5$	56

Three different algorithms were used to deconvolute the CD spectra of Fig. 3: Selcon [24,25] with a data base of 33 proteins; Contin [26] with a data base of 16 proteins; and the K2D neural network algorithm [27].

[a]This number is the sum of β-turn and remainder contents estimated by Contin.

[b]The uncertainty of the values calculated by K2D was 8%, and it is the sum of the maximum uncertainties that were obtained for the contents of α-helix and β-strand.

3.3. p48 is dimeric

The state of association of p48 was checked by size-exclusion FPLC. The elution profile of Fig. 3A shows that a fairly homogeneous preparation was obtained, with the major peak corresponding to an apparent molecular mass of 100 kDa and a Stokes radius of 40 Å. A small peak of higher molecular mass aggregates (~200 kDa) was detected (Fig. 3A) and increased either when refolding was carried out in the absence of DTT (not shown) or upon a 10-fold concentration of the protein in the presence of 3 mM DTT (Fig. 3B, trace 1). Upon addition of 10 mM DTT these aggregates could be fully converted with recovery of the 100 kDa peak (Fig. 3B, traces 2 and 3). The elution position of monomeric

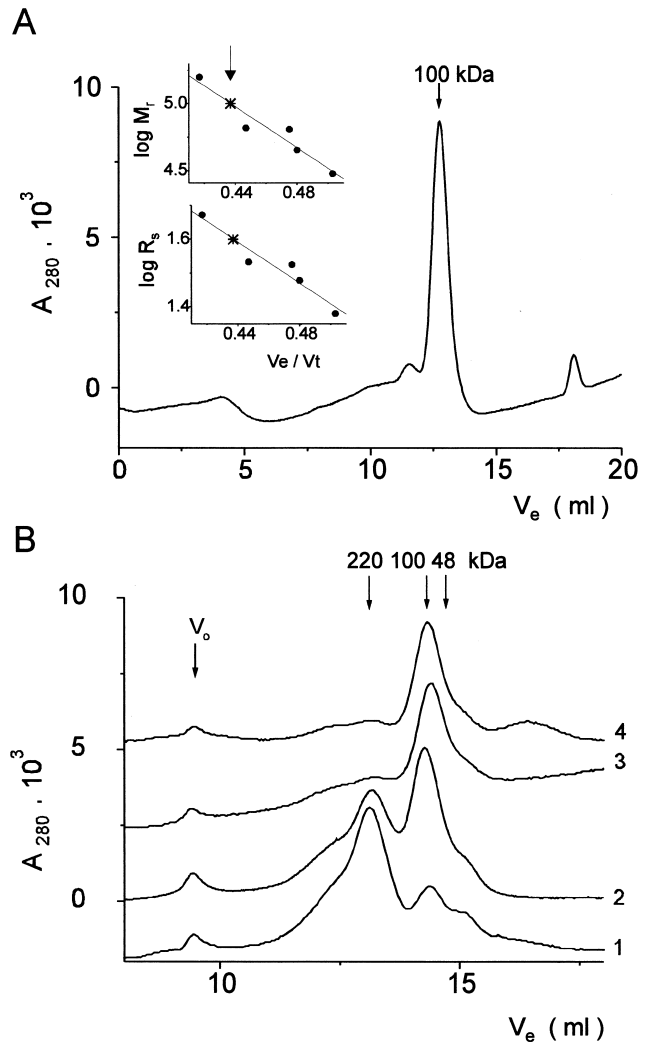

Fig. 3. Size-exclusion FPLC of p48. Profiles of p48 elution in 25 mM phosphate, 0.2 M ammonium sulfate buffer pH 7.5. (A) 0.2 ml of 0.5 mg/ml freshly prepared p48; the insets show the calibration curves that were used to estimate the dependence of molecular mass (M_r, top) or Stokes radius (R_s, bottom) on the fractional volume of elution (V_e/V_t). The star and arrow show the elution position of p48. (B) 25 μl of p48 after 10-fold concentration (trace 1); the same sample 24 h after addition of 10 mM DTT (trace 2), 21 days after addition of 10 mM DTT (trace 3) or, the latter sample after overnight incubation with 200 mM DTT (trace 4).

p48 is indicated in Fig. 3B, and the shoulder in Fig. 3B (trace 3) suggests that a small amount of monomeric protein is present. There was no detectable increase in the proportion of monomeric p48 by increasing the concentration of DTT to 200 mM (Fig. 3B, trace 4) or by a five-fold dilution of the sample (not shown). The results of Fig. 3 indicate that p48 has a strong tendency to self-associate into a 100 kDa dimer and does not depend on intermolecular disulfide bridges. Further association into larger aggregates was negligible under the reducing conditions tested.

3.4. SAXS confirms the dimeric state of p48

p48 was analyzed by SAXS in the absence (Fig. 4A) or in the presence of Mg^{2+} (Fig. 4B). The intensities of scattered rays (I) are plotted as a function of Q^2, which represents the second potency of ($4\pi/\lambda$)

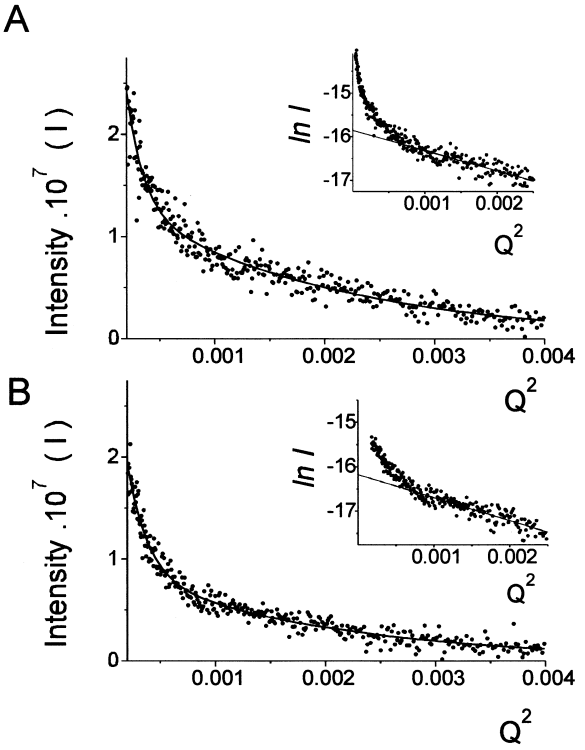

Fig. 4. SAXS measurement of p48. Solutions of 4 mg/ml p48 in phosphate/ammonium sulfate buffer and 200 mM DTT (A) with no additions or (B) plus 50 mM $MgCl_2$ were exposed to X-ray beam of a Synchrotron. Points represent the measured intensity of scattered rays as a function of the different angles of scattering, expressed as Q^2 ($Q = (4\pi \sin\theta)/\lambda$, where 2θ and λ are the scattering angle and the X-ray wavelength, respectively). The solid lines represent fittings with a sum of two exponential decays and were used for calculating radii of gyration (R_g) as described in Section 2. Inset: the data were replotted as $\ln I$ versus Q^2 (Guinier plot), where the two components can be better observed for each case. The solid line in the inset represents a linear regression of the higher angle component, which was used for calculating R_g of p48.

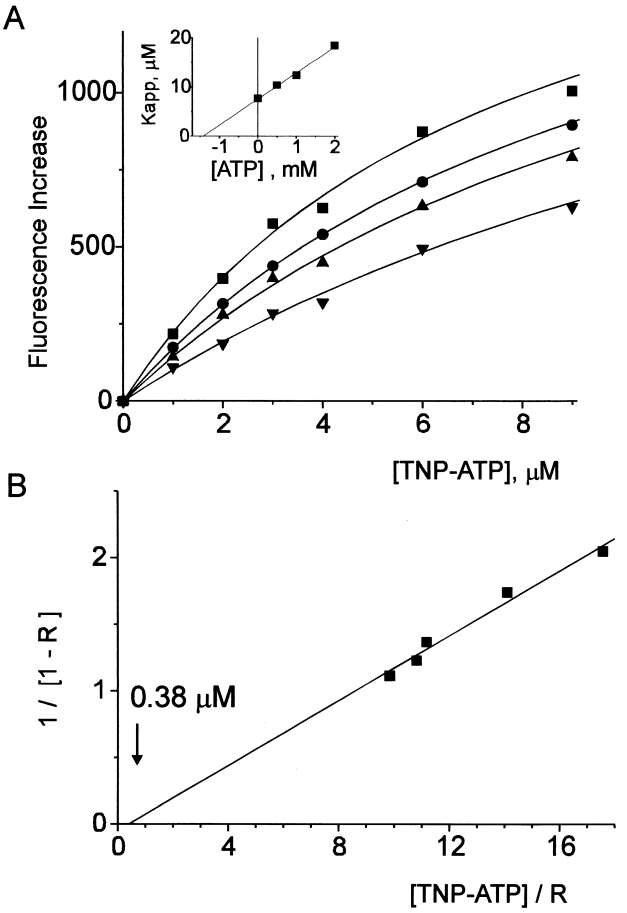

Fig. 5. Binding of TNP-ATP to p48. TNP-ATP binding isotherms were determined by measuring the difference between TNP-ATP fluorescence in the presence of 50 μg p48 (1.05 μM monomer) and in the absence of protein (see Section 2). (A) Fluorescence increase (F) was measured in the presence of different ATP concentrations (0 (■), 0.5 (●), 1 (▲) and 2 (▼) mM ATP) and is represented in an arbitrary scale. The solid lines represent a non-linear fit of data, from where the apparent dissociation constant (K_{app}) and the maximal fluorescence at saturation (F_{max}) were calculated. The inset shows the different K_{app} plotted as a function of ATP concentration. (B) The fraction of fluorescence saturation at each TNP-ATP concentration ($R = F/F_{max}$) in the absence of ATP was calculated and plotted as $1/(1-R)$ versus [TNP-ATP]/R. The concentration of TNP-ATP binding sites of p48 (arrow) can be obtained from the relation $1/(1-R) = K_d^{-1}[\text{TNP-ATP}]/R-(n/K_d)$, according to Gutfreund [35].

$\sin\theta$, θ being the half angle of scattering. Each intensity decay could be fitted with two exponentials (Fig. 4A,B, solid lines) from which two radii of gyration (R_g) could be calculated by the Guinier approximation [31]. The lower R_g component (higher angles of scattering) was found to be 39.2 ± 1.61 and 39.4 ± 1.84 Å in the absence or in the presence of Mg^{2+}, respectively. This component can be better observed by the indicated straight line in the logarithmic plot of the data, in the range of Q^2 between 0.001 and 0.003 (Fig. 4A,B, insets). The R_g value (39 Å) is very similar to the Stokes radius ($R_s = 40$ Å) found for p48 by chromatography (see Fig. 3A), giving a ratio $R_s/R_g = 1.026$. This ratio is significantly below 1.25, which is the expected value for globular proteins [33], indicating that the p48 dimer is not spherical (see Section 4). Again, the particle size obtained by X-ray scattering was compatible with a dimeric structure for p48.

The high R_g component derived from the second exponential in the fittings (Fig. 4A,B) gave $R_g = 126$–141 Å, which can be attributed to the minor amounts of large aggregates of p48 present (see Fig. 3B, traces 3 and 4). Larger mass/size particles are known to dominate the scattering distribution at very small angles [34]. As intensity is proportional to the second potency of R_g, only small amounts of aggregates are enough to contribute a large portion of the intensity decay.

3.5. TNP-ATP binds with high affinity to half of the p48 subunits

TNP-ATP binding was measured by the difference in fluorescence intensity (F) in the presence as opposed to the absence of protein. p48 bound TNP-ATP with high affinity ($K_d = 7.7 \pm 1.7$ μM) and in competition with ATP (Fig. 5A). The apparent affinity (K_{app}) and maximal fluorescence (F_{max}) were obtained by a non-linear fitting of the data from experiments performed in the presence of either 0, 0.5, 1 or 2 mM ATP (Fig. 5A), assuming a hyperbolic dependence of F on TNP-ATP concentration. Similar F_{max} but different K_{app} values were found for the four curves, indicating competition between TNP-ATP and ATP. The K_i of 1.4 mM for ATP could be calculated by plotting K_{app} as a function of ATP (Fig. 5A, inset).

A total of 0.38 mol of nucleotide sites/mol of p48 polypeptide chain was calculated (Fig. 5B) by linearizing the hyperbolic TNP-ATP binding data from Fig. 5A in the absence of ATP [35]. Values varying between 0.24 and 0.64 mol of nucleotide sites/mol of p48 polypeptide chain (mean = 0.46 ± 0.13) were

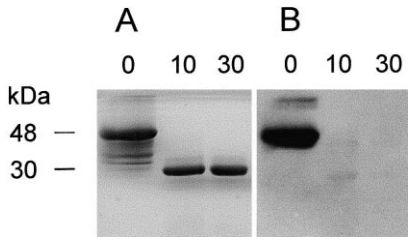

Fig. 6. Proteinase K-digested p48 generates a main 30 kDa fragment. Gels were either (A) stained with Coomassie blue or (B) developed by Western blot with monoclonal antibody anti-Ca^{2+}-ATPase hinge domain (E657–R672). Samples of p48 were digested with proteinase K for 0, 10 or 30 min as indicated and subjected to SDS–PAGE, as described in Section 2. The numbers on the far left indicate the calculated molecular mass of the major bands.

found for eight experiments with five different preparations of p48.

3.6. Digestion of p48 with proteinase K generates a monomeric p30 fragment

Digestion of p48 with proteinase K gave a proteolysis-resistant fragment p30 (Fig. 6A) with similar molecular mass (30 kDa) as that produced by proteinase K treatment of native sarcoplasmic reticulum Ca^{2+}-ATPase [19]. Western blot analysis with monoclonal antibody A52 (against region E657–R672 of native ATPase) revealed that this antibody recognized the p48 peptide (Fig. 6B, lane 0) but did not react with p30 (Fig. 6B, lanes 10 and 30). This result indicates that the p30 fragment was devoid of the hinge domain which corresponds to residues 670–728 in the native protein. In addition, the lack of reactivity of the p30 fragment with anti-hexa-His antibody (not shown) indicated that part of the N-terminal end was also removed by proteinase K.

Size-exclusion chromatography of p30 showed a major peak corresponding to an apparent molecular mass of 34–36 kDa (Fig. 7A) and a Stokes radius $\sim$26.5 Å ($R_{min} \approx 20.6$), indicating that fragment p30 is a monomer, in contrast to the original p48 peptide (Fig. 7B). Binding of TNP-ATP to p30 was assayed in a similar way as described in Fig. 5 and the K_d obtained was 8 μM (not shown).

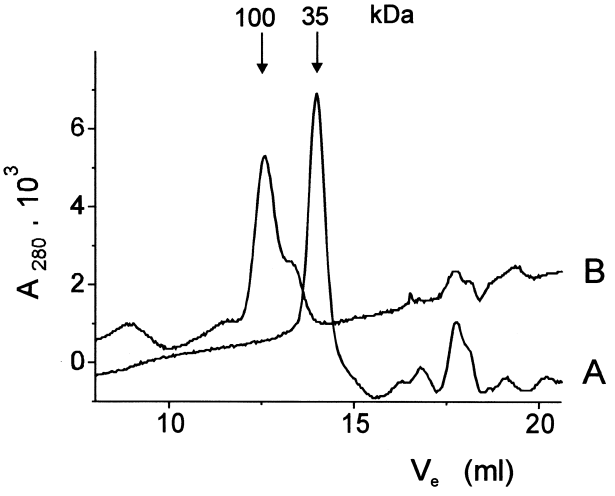

Fig. 7. Size-exclusion FPLC of p30 fragment shows that it is monomeric. Profiles of (A) p30 and (B) p48 elution in 25 mM phosphate, 0.2 M ammonium sulfate buffer pH 7.5, using in both cases a 0.2 ml sample of a solution at 1 mg protein/ml. The arrows show the apparent molecular mass of the major peaks, estimated by referring to a calibration curve.

4. Discussion

The present work shows evidence for an important contribution of the hinge domain of the large hydrophilic fragment of Ca^{2+}-ATPase for self-association into a dimer. Two different methods were used to characterize the dimeric state of the expressed p48, namely filtration chromatography and SAXS. In addition, experimental conditions were optimized to obtain a purified large hydrophilic domain of sarcoplasmic reticulum Ca^{2+}-ATPase exhibiting long-term stability. High yields of protein, in the range of 15–25 mg of purified protein per liter of culture, were obtained. Different salts were tested, and it was observed that the presence of 200 mM ammonium sulfate was essential during refolding to avoid precipitation and permitted concentration of purified samples up to the range of 8–10 mg/ml. Some contaminant proteins of lower molecular mass were present in the preparation, which were eliminated by a gel filtration step following the nickel affinity chromatography. As the contaminants were reactive with Ca^{2+}-ATPase polyclonal antibodies, we believe that they represent degradation products of the domain that retained the His tag. The filtration fractions enriched in these low molecular mass contaminants, in particular one of 38 kDa which represented about 20% of the total protein, was highly insoluble

and precipitated during removal of urea. A strong SH-reducing agent, namely DTT, was required to prevent or even reverse the formation of large aggregates of p48 (Fig. 3B). This behavior was not surprising, as the p48 polypeptide possesses 17 cysteine residues and it is known that no disulfide bonds are required for maintaining the Ca^{2+}-ATPase structure and activity. Purified p48 devoid of the 38 kDa contaminant could be stored at 4°C in the presence of ammonium sulfate and DTT, retaining TNP-ATP binding for up to 4 weeks.

A number of findings in the present report suggest that p48 has a native-like three-dimensional structure. Thus, the pattern of tryptic digestion of p48 is compatible with Arg194 being the most favorable residue for cleavage [18], which is similar to Arg505, the tryptic cleavage point in the native full-length ATPase [16]. Moreover, proteinase K treatment of p48 produced essentially the same p30 fragment described by Champeil et al. [19] for digestion of native ATPase. In addition, deconvolution of CD spectra gave p48 α-helix and β-strand contents similar to those found for the p29/30 peptide, which contains 60% of the large hydrophilic domain [19]. Those values are consistent with the presence of α/β superstructures predicted by a model for native P-type ATPases [14].

The affinities for TNP-ATP and ATP binding to p48 (Fig. 5A) and p30 (not shown) were 4–6-fold lower than those previously described for the 48 kDa cytoplasmic domain expressed in bacteria [17] but only twice lower than the affinity for ATP binding found for the isolated p29/30 peptides derived from proteinase K digestion of native membranes [19]. All the observed nucleotide affinities for the large hydrophilic domain are 5–50-fold lower than for native sarcoplasmic reticulum Ca^{2+}-ATPase. It is conceivable that attachment to the membrane as well as binding to the small cytoplasmic domain may be necessary for the large domain to attain the exact native fold. In this regard, it should be noted that no ATP hydrolysis catalyzed by either p30 or p48 could be detected (not shown). The results shown in Fig. 5B suggest that only half of the p48 polypeptide chains are able to bind TNP-ATP. One possible interpretation is that the subunits in the dimer have non-equivalent affinities for nucleotide. A similar half-the-sites stoichiometry has been described for the p29/30 peptide ATP binding sites [19]. A stoichiometry of 1 mol of TNP-ATP binding sites per mol of expressed cytoplasmic domain has been previously described [17].

Purified p48 was essentially monodisperse as seen by size-exclusion FPLC (Fig. 3A), suggesting a specific state of association for p48 as a dimer of molecular mass around 100 kDa (Stokes radius $R_s = 40$ Å). The molecular mass of p48 calculated from the amino acid composition is 48.4 kDa, thus the theoretical minimum radius for a dimer of $M_r = 96\,800$ is $R_{min} = (3\ M_r\ v/4\pi N)^{1/3} = 30.5$ Å, where $v = 0.74$ cm^3/g [7] and $N = 6.02 \times 10^{23}$. The resulting ratio between measured R_s and calculated R_{min} is 1.31. A spherical globular protein is expected to have $R_s/R_{min} \leq 1.25$ [36], thus suggesting that dimeric p48 is not totally spherical.

SAXS was used as an independent second method to measure the size and shape of p48 in solution. These measurements gave a gyration radius compatible with a predominately dimeric p48 (Fig. 4). It should be noted that Mg^{2+} did not affect the gyration radius. It has been proposed that the hinge domain may be part of a Mg^{2+} binding site [37]. It is clear that whatever may be the effect of Mg^{2+} binding, it did not affect the state of association as measured by SAXS. The ratio between measured values of Stokes (R_s) and gyration (R_g) radii permits one to infer the shape and compactness of the protein in solution [38,39]. This is given by the factor P, which represents the ratio a/b between the semiaxis of revolution of the ellipsoid (a) and its equatorial radius (b). The factor P can be obtained by the relation $R_s/R_g = P^{1/3}[5/(P^2+2)]^{1/2}$. For an ideal spherical structure $a = b$, then $P = 1$ and the above equation gives $R_s/R_g = 1.29$ [33]. We have found for p48 a ratio R_s/R_g of 1.026, giving a P value of 2.67, which suggests that p48 dimer is elongated. In fact, in view of the images obtained for native sarcoplasmic reticulum Ca^{2+}-ATPase by crystallography, an elliptical shape rather than globular is expected for the ATPase monomer [14]. Improved resolution of cryoelectron microscopy of tubular crystals of the Ca^{2+}-ATPase has revealed that ATPase monomers were in face to face contact with each other through the head-shaped hydrophilic domain and that dimer-ribbon structures were present [3]. From the dimensions of the monomeric unit [3,14,40] the dimensions of a

dimeric cytoplasmic portion, comprising stalks and a small loop, can be inferred to be 70 (height)×50 (width)×160 (length) Å. By approximating the latter as an ellipsoid with a 60 Å average equatorial diameter and a 160 Å axis of revolution, a *P* value of 2.67 is obtained, which is identical to the *P* value of 2.67 experimentally found for p48.

A dimeric arrangement for the Ca^{2+}-ATPase has been proposed for a long time. The original evidence came from the observation of a biphasic dependence on ATP concentration for ATP hydrolysis [5]. Saturation-transfer electron paramagnetic resonance methods support the involvement of changes in the dimeric arrangement during catalysis [10]. More recently, a dimeric structure has been proposed from interpretation of infrared spectra of the native Ca^{2+}-ATPase at different temperatures [11], but a tetrameric structure has also been proposed to explain the behavior of the phosphatase activity of the enzyme in view of the E1-E2 model [41].

The data presented in this paper suggest the involvement of the large hydrophilic domain for self-association of Ca^{2+}-ATPase monomers into a dimer, and point to the crucial role of the hinge domain in this phenomenon. The hinge domain was shown to be absent in the C-terminal end of monomeric p29/30 [19], which lacks 133 amino acids (I611–I743 in the full-length ATPase) that are present in the C-terminal end of the p48 fragment obtained in the present work. In analogy, the shorter p30 monomeric fragment obtained in the present work by proteinase K digestion does not contain the A52 epitope region (E657–R672) [23], therefore lacking at least 87 amino acids from the C-terminal end when compared to p48. The missing C-terminal end comprises the conserved hinge domain (residues 670–728) [42]. Thus, it is attractive to suppose that the conserved hinge domain contained in dimeric p48 but absent in monomeric p30, in particular the conserved motif ^{702}GDGVND^{707}, might be the determinant for dimerization. However, the hinge domain might not be directly involved in dimerization, as the removal of this region might modify the rest of the large hydrophilic domain, including sequences actually involved in dimerization. It is possible that dimerization of the hydrophilic domain might be representative of the tendency of native sarcoplasmic reticulum Ca^{2+}-ATPase to associate as a dimer in the membrane. In this regard, mutations in the conserved motif of the hinge domain, particularly the aspartyl residues, have indicated that the conserved amino acids in the hinge domain are required for the activity of the full-length membrane-bound ATPase [42]. Although it has been reported that monomeric Ca^{2+}-ATPase is fully active [12], the kinetic characteristics of monomeric Ca^{2+}-ATPase have not been determined in detail. The present work suggests the need for further studies on hinge motif mutants to clearly establish the role of the hinge domain on self-association of the full-length ATPase and on its catalytic activity. These studies must, however, await further developments in the heterologous expression systems, which at present can only provide recombinant full-length Ca^{2+}-ATPase with 3–5% purity [16,20,42,43].

Acknowledgements

This work was supported by a grant from Fundação de Amparo a Pesquisa do Estado de São Paulo, FAPESP, and by Conselho Nacional para o Desenvolvimento Científico e Tecnológico, CNPq. We thank Dr. Iris Torriani for help in analyzing the SAXS measurements performed at LNLS-National Synchrotron Light Laboratory, Brazil, and Dr. D.H. MacLennan, Toronto, Canada, for providing the cDNA clone of SERCA1 and monoclonal antibody A52. P.C.C.A. was on leave from Universidade Federal do Rio de Janeiro and received a visiting fellowship from FAPESP.

References

[1] G. Inesi, Annu. Rev. Physiol. 47 (1985) 573–601.
[2] D.H. MacLennan, C.J. Brandl, B. Korczak, N.M. Green, Nature 316 (1985) 696–700.
[3] C. Toyoshima, H. Sasabe, D.L. Stokes, Nature 362 (1993) 469–471.
[4] D.L. Stokes, P. Zhang, C. Toyoshima, K. Yonekura, H. Ogawa, M.R. Lewis, D. Shi, Acta Physiol. Scand. 643 (Suppl.) (1998) 35–43.
[5] G. Inesi, J.J. Goodman, S. Watanabe, J. Biol. Chem. 242 (1967) 4637–4643.
[6] J.A. Reynolds, E.A. Johnson, C. Tanford, Proc. Natl. Acad. Sci. USA 82 (1985) 3658–3661.
[7] M. LeMaire, J.V. Moller, C. Tanford, Biochemistry 15 (1976) 2336–2342.

[8] J.L. Silva, S. Verjovski-Almeida, Biochemistry 22 (1983) 707–716.
[9] J.L. Silva, S. Verjovski-Almeida, J. Biol. Chem. 260 (1985) 4764–4769.
[10] J.E. Mahaney, J.P. Froehlich, D.D. Thomas, Biochemistry 34 (1995) 4864–4879.
[11] I. Echabe, U. Dornberger, A. Prado, F.M. Goni, J.L. Arrondo, Protein Sci. 7 (1998) 1172–1179.
[12] M. LeMaire, A. Viel, J.P. Moller, Anal. Biochem. 177 (1989) 50–56.
[13] J.P. Froehlich, K. Taniguchi, K. Fendler, J.E. Mahaney, D.D. Thomas, R.W. Albers, Ann. NY Acad. Sci. 834 (1997) 280–296.
[14] N.M. Green, D.L. Stokes, Acta Physiol. Scand. 607 (Suppl.) (1992) 59–68.
[15] E. Mintz, F. Guillain, Biochim. Biophys. Acta 1318 (1997) 52–70.
[16] N.M. Green, D.H. MacLennan, Biochem. Soc. Trans. 17 (1989) 819–822.
[17] M.J. Moutin, M. Cuillel, C. Rapin, R. Miras, M. Anger, A.M. Lompré, Y. Dupont, J. Biol. Chem. 269 (1994) 11147–11154.
[18] M.J. Moutin, C. Rapin, R. Miras, M. Vincon, Y. Dupont, D.B. McIntosh, Eur. J. Biochem. 251 (1998) 682–960.
[19] P. Champeil, T. Menguy, S. Soulie, B. Juul, A.G. deGracia, F. Rusconi, P. Falson, L. Denoroy, F. Henao, M. le Maire, J.V. Moller, J. Biol. Chem. 273 (1998) 6619–6631.
[20] K. Maruyama, D.H. MacLennan, Proc. Natl. Acad. Sci. USA 85 (1988) 3314–3318.
[21] O. Lowry, N. Rosebrough, R. Farr, R. Randall, J. Biol. Chem. 193 (1951) 265–275.
[22] E. Harlow, D. Lane, Antibodies: A Laboratory Manual, Cold Spring Harbor Laboratory Press, Cold Spring Harbor, NY, 1988.
[23] D.M. Clarke, K. Maruyama, T.W. Loo, E. Leberer, G. Inesi, D.H. MacLennan, J. Biol. Chem. 264 (1989) 11246–11251.
[24] N.J. Greenfield, Anal. Biochem. 235 (1996) 1–10.
[25] N. Sreerama, R.W. Woody, Anal. Biochem. 209 (1993) 32–44.
[26] S.W. Provencher, J. Glöckner, Biochemistry 20 (1981) 33–37.
[27] M.A. Andrade, P. Chacón, J.J. Merolo, F. Morán, Protein Eng. 6 (1993) 383–390.
[28] B. Rost, C. Sander, Proteins 19 (1994) 55–72.
[29] P.Y. Chou, G.D. Fasman, Biochemistry 13 (1974) 222–245.
[30] V.N. Uversky, Biochemistry 32 (1993) 13288–13298.
[31] A. Guinier, Ann. Phys. 12 (1939) 161–237.
[32] D.A. Thorley-Lawson, N.M. Green, Biochem. J. 167 (1977) 739–748.
[33] K. Gast, H. Damaschun, R. Misselwitz, M. Muller-Frohne, D. Zirwer, G. Damaschun, Eur. Biophys. J. 23 (1994) 297–305.
[34] A. Guinier, G. Fournet, Small Angle X-ray Scattering, John Wiley and Sons, New York, 1955.
[35] H. Gutfreund, in: Enzymes, Physical Principles, Wiley-Interscience, London, 1972, p. 71.
[36] C. Tanford, Y. Nozaki, J.A. Reynolds, S. Makino, Biochemistry 13 (1974) 2369–2376.
[37] J.L. Girardet, I. Bally, G. Arlaud, Y. Dupont, Eur. J. Biochem. 217 (1993) 225–231.
[38] T.F. Kumosinski, H. Pessen, Methods Enzymol. 117 (1985) 154–182.
[39] L. Shi, M. Kataoka, A.L. Fink, Biochemistry 35 (1996) 3297–3308.
[40] P. Zhang, C. Toyoshima, K. Yonekura, N.M. Green, D.L. Stokes, Nature 392 (1998) 835–839.
[41] J. Nakamura, G. Tajima, J. Biol. Chem. 272 (1997) 19290–19294.
[42] B. Vilsen, J.P. Andersen, D.H. MacLennan, J. Biol. Chem. 266 (1991) 16157–16164.
[43] E.M.R. Reis, E. Kurtenbach, A.R. Ferreira, P.J.C. Biselli, C.W. Slayman, S. Verjovski-Almeida, Biochim. Biophys. Acta 1461 (1999) 83–95.